Hindawi Publishing Corporation
Advances in Materials Science and Engineering
Volume 2014, Article ID 180193, 10 pages
http://dx.doi.org/10.1155/2014/180193

Research Article

Seismic Behavior of Short Concrete Columns with Prestressing Steel Wires

Deng Zong-Cai, Jumbe R. Daud, and Li Hui

The Key Laboratory of Urban Security and Disaster Engineering, Ministry of Education, Beijing University of Technology, Beijing 100124, China

Correspondence should be addressed to Deng Zong-Cai; dengzc@bjut.edu.cn

Received 21 February 2014; Revised 9 June 2014; Accepted 10 June 2014; Published 5 August 2014

Academic Editor: Yucel Birol

The seismic behavior of short circular reinforced concrete columns was studied by testing seven columns retrofitted with prestressing steel wire (PSW), subjected to combined constant axial compression and lateral cyclic load. The main test parameters were configuration index of PSW, prestressing level of PSW, and axial compression ratio. An analysis and discussion of the test results including failure mode, hysteresis curves, skeleton curves, ductility, and degradation of stiffness was done. The results show that the seismic performance of the retrofitted specimens could be effectively enhanced even if the axial compression ratio of columns reached 0.81. The ductility index and the energy absorption capacity of the retrofitted specimens increase with the prestressing level of PSW. The formulas for calculating shear capacity of RC short columns strengthened with PSW were proposed which may be useful for future engineering designs and researches.

1. Introduction

Many of the catastrophic failures of bridges or frame structures that occurred during the past earthquakes were due to the failure of one or more of the RC columns. Shear damage sustained by short and stubby columns is often responsible for the collapse of the entire structure. The deficiencies in the seismic shear resistance may be attributed to the old design provisions, which resulted in lack of sufficient transverse reinforcement. This deficiency may still be found in some of the more recently designed columns. While lack of adequate transverse reinforcement may lead to diagonal tension failure in shear dominant columns [1].

A large number of existing bridge columns or frame columns are also susceptible to anchorage failure because of the location of longitudinal reinforcement splices, which often coincide with potential plastic hinges regions. Lack of flexural ductility problem is common in the bridge piers or short frame columns, which arises from two sources: (1) insufficient transverse reinforcement that results in lack of adequate confinement and (2) inadequate lap splice length in the plastic hinge zone. Such events motivated many researchers to do study on the reason behind RC bridge columns failure during earthquakes.

It has also been proven that the ductility capacity of columns is enhanced significantly when the core concrete is well confined. Passive confinement of concrete using external steel jackets or fiber reinforced polymers (FRPs) wrapping is the most common method used to improve the ductility capacity of the columns [2, 3]. Although the passive confinement has been widely used around the world, researches have shown that better results can be obtained by using external pressure on the concrete column which is also called active confinement.

There have been a number of studies that attempted to explore the feasibility of using active confinement for seismic retrofit of concrete columns. Seismic behaviors and compressive strength of square cross section RC columns retrofitted with prestressed CFRP and AFRP strips was researched [4]. Other studies focused on exploring the effect of active confinement on the material level test [5]. This method of retrofitting has already been used in retrofitting projects. Some of researchers [6] studied a new technique of using active confinement on concrete columns by metal strips. The results showed significant increase in the strength and ductility of specimens due to active confinement by metal strips. Prestressed high-strength steel strips were used in the

retrofitting of quadratic columns in order to improve the seismic performance of concrete columns [7, 8], in which the crack propagation was greatly reduced and the general seismic performance was promoted.

University of Ottawa [9] conducted a research on the shear behavior of concrete columns retrofitted by prestressed steel wires, in which results showed that prestressing can suppress shear failure and significantly improve the shear behavior of RC columns, but during construction, each strand had to be anchored with nails fixed onto the surface of existing concrete member and tension applied using a feed through tensile jack, which makes construction process complex.

The authors therefore developed a new type of prestressing anchoring system for retrofitting concrete column with high-strength steel wires [10, 11]. In this paper, experimental research and theoretical analysis of the seismic performance of retrofitted RC short column using prestressed steel strands have been conducted. Seven prestressed strands retrofitted short columns and 1 control columns were prepared, investigated the influence of axial compression ratio, spacing of steel strands and prestress level on the seismic performance of short RC columns. The formula for calculating the shear capacity of prestressed steel strands retrofitted columns is suggested. From the findings it is observed that applying this new tension and anchoring technology can significantly improve the seismic behavior of short concrete columns; no damage to the retrofitted member is caused; the construction process is simple and easy and saves cost and operation space, no need for special surface treatment of the existing concrete columns; good corrosion resistance is achieved and simplifies on-site construction.

2. Experimental Design

2.1. Specimen Design and Retrofitting Program. The diameter of RC cylindrical columns is 300 mm and of height 430 mm. The column is prepared using C35 concrete. Vertical casting is applied, where first the ground beam is cast then three weeks later the column and column head are cast. The circular cross section column template is made using PVC pipe; ground beams and column head are cast in wooden templates.

The mixing ratio for the C35 concrete is cement 311 kg/m^3, sand 854 kg/m^3, gravel 1035 kg/m^3, water 170 kg/m^3, ordinary Portland cement PO.42.5, medium sand, and maximum size of gravel particle 25 mm. The mixing ratio for the epoxy polymer mortar is cement 711 kg/m^3, sand 1434 kg/m^3, water 340 kg/m^3, polypropylene fiber 2.1 kg/m^3, epoxy polymer 2.7 kg/m^3, ordinary Portland cement PO.42.5, and medium sand.

Three cubic specimens and three prismatic specimens were prepared for concrete and polymer mortar under the same conditions with columns, to test the compressive strength of the concrete and mortar. The tested compressive strength of the cubic and prismatic concrete specimens at 40 days is 41.5 MPa and 33.0 MPa, respectively; the compressive strength of the polymer mortar is 53.60 MPa. The nominal diameter of the steel strands is 4.5 mm and cross section area

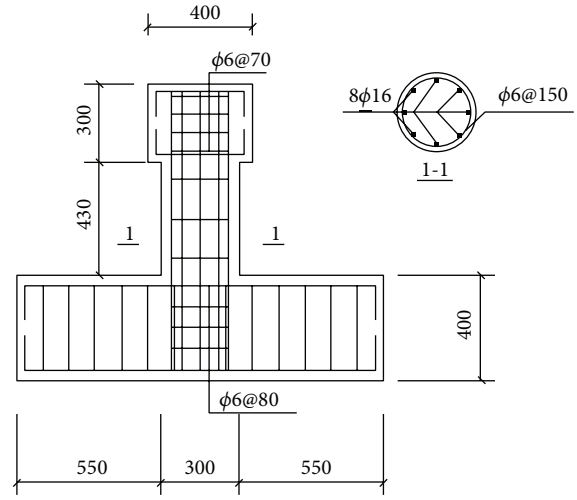

Figure 1: Details of the specimens.

is 9.62 mm^2, the proportional and ultimate tensile strengths of strands are 1320 MPa and 1750 MPa, respectively. The stirrup grade is HPB235, of diameter 8 mm, yield tensile strength 407.3 MPa, and ultimate tensile strength 459.0 MPa. Longitudinal rebar is HRB335, of diameter 16 mm, yield tensile strength 385.3 MPa, and ultimate tensile strength 537.3 MPa. The curing age is 40 days and curing is done at room temperature for all columns, cubic and prismatic concrete specimens.

Shear span ratio of column is H/h, where H is the height of the column and h is the height of cross section column. The volumetric ratio of stirrup reinforcement of the columns is obtained by calculating the ratio of the amount of stirrup reinforcement to a unit volume of concrete; that is, volume of concrete is obtained by calculating a part of concrete column of height s_p, where s_p is stirrup spacing.

In the experiment, 8 circular cross section short columns were designed, of which 7 were retrofitted and one control specimen. Specimen shear span ratio is 1.93, volume ratio of stirrup reinforcement is 0.25%, and longitudinal reinforcement ratio is 2.28%. Specimen geometry and reinforcement details are shown in Figure 1.

The variables include 4 different prestressing levels, 3 different strand spacing measurements (30 mm, 60 mm, and 90 mm) and 3 different design axial compression ratios (0.6, 0.81, and 0.9). Design axial compression ratios $n = N/f_cA$, f_c is design axial compressive strength of concrete prismatic specimen and A is the area of cross section for column.

The retrofitting setup and strand tensioning anchoring are shown in Figure 2. The apparatus comprises two steel plate anchors and high-strength bolts [10], which are used for prestressing; one end the steel strand is fixed to a steel plate anchor, looped around a concrete column; then the other end is fixed to another steel plate anchor. Prestressing of the steel strands is done and controlled by tightening and loosening of the bolt. First grind to smoothen, flatten, and remove loose particles from the column specimens then clean and polish the column surface using acetone. Set the already

Figure 2: Circular columns prestressed with steel wires.

Figure 3: Test setup.

Table 1: Test parameters.

Specimen number	Design axial compression ratio n	Strands spacing (mm)	λ_{sw}	α
PZ1	0.81	—	—	—
PZ2	0.81	30	0.237	0
PZ3	0.81	30	0.237	0.30
PZ4	0.81	30	0.237	0.40
PZ5	0.81	30	0.237	0.50
PZ6	0.60	60	0.119	0.40
PZ7	0.81	60	0.119	0.50
PZ8	0.90	90	0.079	0.65

prepared steel strands and steel plate anchors in position and tighten the high-strength bolts to induce tension in the steel strands hooped around the column for pretensioning. Brush with concrete interface agent and after hardening smear 2 cm thick polymer mortar and wrap with plastic film for curing. The labeling of specimens and test parameters are shown in Table 1.

Strands configuration value $\lambda_{sw} = \rho_{psw} f_{sw}/f_c$, where ρ_{psw} is volumetric ratio of the strand stirrup, which is similar to volumetric stirrup ratio; f_{sw} is the tensile strength of the strand; f_c is the compressive strength of concrete; α is prestress level, the ratio between strand tension strain and ultimate strain of retrofitting strands.

2.2. Experiment Apparatus and Loading System. Loading setup is shown in Figure 3. The vertical load at the top of the column is applied using a hydraulic jack, which is controlled using the hydraulic servo system. A sliding roller is installed between capital the jack and beams to ensure that the column top moves freely horizontally, and through the entire experiment the vertical force remains constant. Horizontal load is applied using tension and compression jack fixed on reaction wall.

Force or displacement control method is applied. Horizontal loading is by load or displacement control method: before yielding of the longitudinal reinforcement, load control is applied, where the loading level increased after each loading cycle. After yielding, the displacement control method is adopted, where the displacement value just as the longitudinal reinforcement yields is taken as the displacement control value for each loading stage, where loading is twice for each cycle. When the horizontal load drops to 85% of the ultimate load, the specimen has attained failure load and deformation; therefore the test is terminated.

2.3. Measurements. The value of axial load and horizontal cyclic load is measured by the force sensor. A dial indicator is fixed on the foundation beam to measure the foundation horizontal displacement, two rod displacement meters attached the top of the column side, take the difference between the mean displacement at the top and bottom of the beam as the final column displacement under horizontal loading.

Paste strain gages on the column longitudinal reinforcement and stirrups to measure the strain. For retrofitted column, apart from longitudinal reinforcement and stirrups strain gages, others are also attached on the steel strands to measure the strand strain under horizontal load. Horizontal load and displacement as well as all the data are recorded by computer-controlled data acquisition system.

3. Experimental Results and Analysis

3.1. Failure Process. The main parameters of each specimen like design axial compression ratio, strand stirrup configuration index, and prestressed levels vary, hence cracking and failure modes are not the same. Typical specimen failure pattern is shown in Figure 4 and summarized below.

(1) Specimen PZ1 (Unretrofitted Column, $n = 0.81$). At initial loading, the specimen exhibits elastic characteristics; after unloading there is no significant residual deformation. When horizontal load reaches 250 kN, the first horizontal crack appears near the axis of the column about 100 mm from the top surface of the column. Once horizontal loading increases to 300 kN, diagonal cracks form at $3/4h$ extending rapidly (h is net height of the pillar and observation point is determined from the top surface) to $1/3h$ of the column on one side, at the same time several diagonal cracks can be observed on the other side of the column. Horizontal cracks appear at the bottom and gradually propagate to both sides of the column. When the horizontal load reaches 340 kN, horizontal cracks increase and later become flexure-shear cracks, causing more

(a) PZ1 (b) PZ2 (c) PZ3 (d) PZ4

(e) PZ5 (f) PZ6 (g) PZ7 (h) PZ8

Figure 4: Failure patterns of specimens.

diagonal cracks to appear; the protective layer at the column base crushes slightly, followed by yielding of longitudinal reinforcement and rapid expansion of cracks. At displacement control testing stage stirrup strain increases rapidly, the diagonal cracks widen rapidly, and a clear concrete bulge is seen at the column bottom. A decrease in horizontal force bearing capacity follows and peeling of concrete is observed. At this stage the specimen is considered destroyed and the test is terminated.

(2) Retrofitted Specimen PZ2 (Nonprestressed Steel Strand, $n = 0.81$, $\lambda_{sw} = 0.237$, *and* $\alpha = 0$*).* At initial loading no significant changes on the specimen are observed. When horizontal loading attains 300 kN, the first horizontal central crack on the polymer mortar layer at the pushing side appears; at 340 kN of loading, horizontal cracks appear on mortar layer at $1/3h$ at the pull side; as load increases, the horizontal cracks gradually extend to the column base. When loading attains 360 kN, longitudinal reinforcements yield, turning points can be seen on the force-drift curve, and residual deformation increases after unloading, indicating that the column has begun to enter the stage of elasto-plastic deformation; disintegrating sound of polymer mortar layer can be heard. At $+2\Delta_y$ (2.88% drift) (the first loading cycle at twice the yield displacement, "+" represents a push and "−" represents a pull), existing cracks continue to extend and widen and new diagonal cracks begin to form; at $-2\Delta_y$ (−2.8% drift), intersecting cracks form at $1/3h$, and the mortar layer at the column base begins to disintegrate. At $-3\Delta_y$ (−4.2% drift), column mortar layer peels off at about $1/3h$ area. Knocking the polymer mortar layer one can hear "a hollow sound," which indicates the mortar layer has disintegrated from the concrete column. Horizontal displacement increases steadily. At $\pm 4\Delta_y$ (5.6% drift), the lower part of the specimen expands laterally, the "hollowness" increases, and the curve reflects declining bearing capacity. When the test is terminated, the polymer mortar layer peels off, bending cracks at the bottom of the column appear to be denser and more than those of a standard column, many short diagonal cracks branch out, and the steel strands loosen.

(3) PZ3, PZ4, and PZ5 Specimens (α *Is Different for Each Specimen, While Other Parameters Remain the Same,* $n = 0.81$, $\lambda_{sw} = 0.237$*).* At initial loading of PZ3 with $\alpha = 0.30$, no significant changes are seen. When loading attains 320 kN, at 130 mm from the column top, a 150 mm long horizontal crack appears; horizontal displacement at the top of the columns attains 8 mm; longitudinal tensile reinforcement yields; the section stiffness reduces suddenly. At $+2\Delta_y$ (2.4% drift), more diagonal cracks appear on the sides of PZ3 specimen and gradually get across; at $-2\Delta_y$ (−2.8% drift) horizontal cracks appear at the column base, while existing horizontal cracks extend rapidly and several vertical cracks appear on the column bottom mortar surface; at $+4\Delta_y$ (5.6% drift) a large area of the mortar layer disintegrates from the concrete column. After the test, due to disintegrating of mortar layer it is observed that the column bottom concrete begins to crush exhibiting flexural failure characteristics.

Specimens PZ4 ($\alpha = 0.40$) and PZ5 ($\alpha = 0.50$) failure process is similar to that of PZ3. Compared to PZ3 the diagonal cracks of the two specimens are finer and denser, load bearing capacity decrease is slower, and lateral expansion of concrete columns is less. Knocking off the mortar layer to compare the three specimens, it was found that the higher the level of strand prestressing is, the more the strands strain is, the lesser the degree of damage is, and the more significant flexural failure characteristics are.

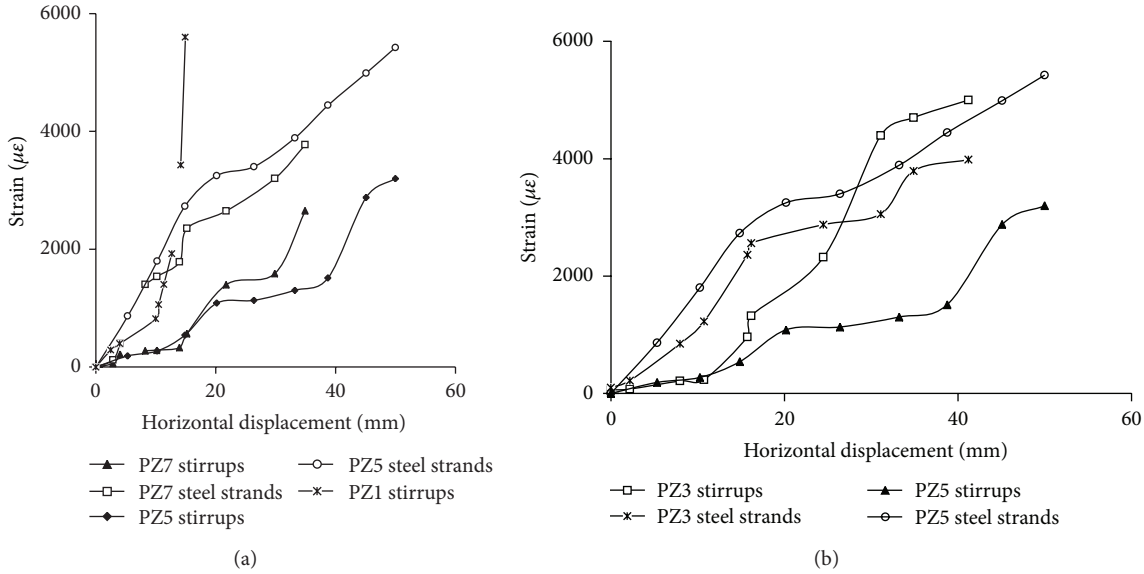

Figure 5: Comparison of strains in stirrups and steel wires.

(4) The Specimens PZ6, PZ7 (Both with Equal Strand Configuration Index $\lambda_{sw} = 0.119$) and Specimen PZ8. When horizontal load is 320 kN, the first horizontal crack appears on specimen PZ7 ($n = 0.81, \alpha = 0.50$) on the push side at $1/3h$; at −320 kN a crack about 100 mm long appears at the midheight on the other side of the column, and this time horizontal cracks gradually extend diagonally. When horizontal load is approximately 370 kN longitudinal reinforcement suddenly yields, diagonal cracks quickly extend and widen, and mortar layer and concrete produce peeling sound. At $2\Delta_y$ (2.53% drift) a diagonal crack at $2/3h$ extends to the column bottom and cracking sound becomes louder. At $-5\Delta_y$ (−6.3% drift) loud bangs can be heard twice, concrete lateral expansion increases, mortar layer peeling off becomes more significant, and the test ends. Knocking off polymer mortar layer, it is found that the second to the fifth strands (counted from the column bottom upwards) are fractured. The third, fourth, and fifth steel strands are at the diagonal cracks area. The column bottom concrete crushed significantly, horizontal and diagonal cracks crossed, indicating bending-shear failure characteristics.

The specimen PZ6 ($n = 0.6, \alpha = 0.40$) failure process is similar to PZ7, but the former has less concrete lateral expansion, steel strands do not rupture, and bending cracks can be seen at the bottom of the column.

The failure process of specimen PZ8 ($n = 0.9, \lambda_{sw} = 0.079, \alpha = 0.65$) is similar to PZ7 at initial loading stage, but different at later loading stages. The bearing capacity of the former decreases faster, diagonal cracks extend rapidly, and horizontal crack spacing is larger. During failure the steel strands do not rupture and horizontal displacement is small. This indicates that when the strands spacing is large, increasing the prestress of the strands still does not produce better constraints to the core concrete.

3.2. Stirrups and Strands Strain. Throughout the experiment the steel wires work normally during loading, since the anchorage system is highly efficient and reliable. For the retrofitted specimens, the lateral expansion of the concrete is contained by the steel strands and stirrups such that the deformation capacity of the specimen is significantly improved. Concrete confining effect can be reflected by the respective specimen's strands tensile strain level. The specimens stirrups and strands strain are compared by recording the second stirrup strain (180 mm from the column top surface) and the strand corresponding to stirrup's position. Figure 5 is a typical specimen stirrups and strand strain comparison chart.

From Figure 5(a) it can be seen that, at initial loading stages, stirrups strain increase in the control column is slow, until displacement is greater than 7 mm when diagonal cracks appear. After yielding of the stirrups, strain increases rapidly. Before appearance of diagonal cracks on prestressed steel strands retrofitted columns, stirrups strain is small, but when cracks appear there is a sudden increase in the stirrups strain and with time the increase rate rises. Under equal horizontal displacement, the stirrups strain in prestressed retrofitted column is far less than the corresponding control columns. At the same degree of displacement, as the strand configuration index increases (strand spacing reduces), stirrups strain displays a decreasing trend, while strands strain shows an increasing trend. When specimens with higher prestress level (PZ5 and PZ7) are under equal horizontal displacement, the strands strain value is significantly greater than the stirrups strain, indicating that, with increased displacement, the stirrup constraints on the concrete and shear resistance are gradually shared by the steel strands. And the larger α and λ_{sw} are, the earlier the strands get subjected to force, and thus the greater the shared horizontal force is.

With other parameters remaining equal, the specimens with lower prestressed level, stirrups strain increases

Table 2: Test results of key points in P-Δ curves.

Specimen number	Load (kN)			Displacement (mm)		ductility		Failure mode
	P_y	P_m	P_u	Δ_y	Δ_u	μ	Increase (%)	
PZ1	337.1	368.0	312.8	6.07	20.4	3.36	—	Shear
PZ2	359.7	405.0	344.3	8.09	39.9	4.93	33.6	Bending shear
PZ3	376.7	419.3	356.4	7.02	41.14	5.86	74.4	Bending
PZ4	382.5	431.1	366.4	5.15	32.20	6.25	86.0	Bending
PZ5	389.0	419.8	356.8	7.52	48.46	6.44	91.7	Bending
PZ6	367.0	381.4	324.2	6.74	37.56	5.57	65.6	Bending
PZ7	385.0	408.5	347.2	7.33	37.09	5.06	50.6	Bending shear
PZ8	397.9	451.2	383.5	6.75	25.60	3.71	10.4	Bending shear

Note: due to equipment failure during the loading process of specimen PZ5, resulting in larger axial pressure fluctuations, the measured horizontal load is small.

rapidly; these specimens stirrups strain value is significantly higher than specimens with high prestress level, as seen in Figure 5(b). When horizontal displacement is 15.5 mm, the stirrups yield in specimens PZ3 ($\alpha = 0.30$) with lower prestress level, while specimens PZ5 ($\alpha = 0.50$), with higher prestress level, recorded stirrups strain only 650 $\mu\varepsilon$, and at the same loading cycle the stirrups strain of PZ3 is always larger than of PZ5.

3.3. Hysteresis Curve. The measured force-drift typical hysteresis curve is shown in Figure 6.

From Figure 6 we see the following.

(1) Before yielding, the area under the force-drift hysteresis curves of all specimens is small, and after unloading the residual deformation is very small. After yielding, increase in loading cycles and the horizontal displacement leads to significantly reduced force-drift curve slope. After unloading residual deformation gradually increases, which indicates that the stiffness of the specimen is deteriorating.

(2) Once reaching displacement control loading stage, the unretrofitted column PZ1 undergoes shear failure, hysteresis loop at elastic-plastic phase takes an arched shape, and pinching of the curve is observed, which displays shear deformation characteristics and poor seismic performance.

(3) By applying prestressed steel strand retrofitting, hysteresis loop is generally plumped; ductility and energy dissipation capacity are good.

(4) Comparing the force-drift curves of PZ1, PZ2, PZ3, and PZ4 specimens, it can be seen under the same λ_{sw} and axial compression ratio, as the strand prestressing level is increased, the specimen hysteresis loop becomes more plumped and the seismic performance is also improved.

(5) Under the same axial compression ratio and strand prestressing level (for specimens PZ5 and PZ7), increasing λ_{sw} changes the specimens failure mode from flexural-shear failure to better ductile flexural failure, and a more plumped hysteresis loop is obtained.

(6) As the axial compression ratio increases, the hysteresis curve becomes relatively narrow. After yielding of the specimen there is significant strength and stiffness degradation. The greater the displacement, the more the strength and stiffness degradation. At later loading stages, the force-drift curve becomes more unstable.

3.4. Skeleton Curve. The specimen's P-Δ skeleton curve is shown in Figure 7.

The characteristics of each specimen (load point and displacement) are listed in Table 2, where P is horizontal force, Δ is horizontal displacement corresponding to horizontal loading point, and Δ_y is the yield displacement corresponding to the yield load P_y; P_y is defined as the point, where the curve begins to bend, Δ_m is displacement corresponding to the peak load P_m and Δ_u is the displacement corresponding to the ultimate load P_u.

From Figure 7 it is observed that the skeleton curve of each specimen can be divided into elastic stage, ascending stage, and descending stage. At elastic stage, the skeleton curve for each specimen takes the same form, indicating that the effects of prestress level and confinement at elastic stage are little.

After yielding prestressing steel strands reinforced columns exhibit good carrying capacity; after peak load, the skeleton curve enters a horizontal stage and a gentle descending stage, and seismic performance is effectively improved. Compared with the control column, nonprestressed steel strand retrofitted column PZ2 displays improved deformation, but at late loading stage skeleton curve decreases rapidly and the descending segment is shorter. For lower strand configuration index specimen PZ8, though strand prestressed level is high, due to high axial compression ratio, descending stage exhibits sharp decline and bending-shear failure. When steel strand configuration index is too low, the prestressing effect on improving the seismic performance of short columns with high axial compression ratio is not significant. Under high axial compression ratio ($n = 0.81$), deformation properties of specimens with strand configuration index 0.237 (PZ2, PZ3, PZ4, and PZ5) improve with increase in strand prestressing level. Comparing PZ2, PZ3, PZ4, and PZ7,

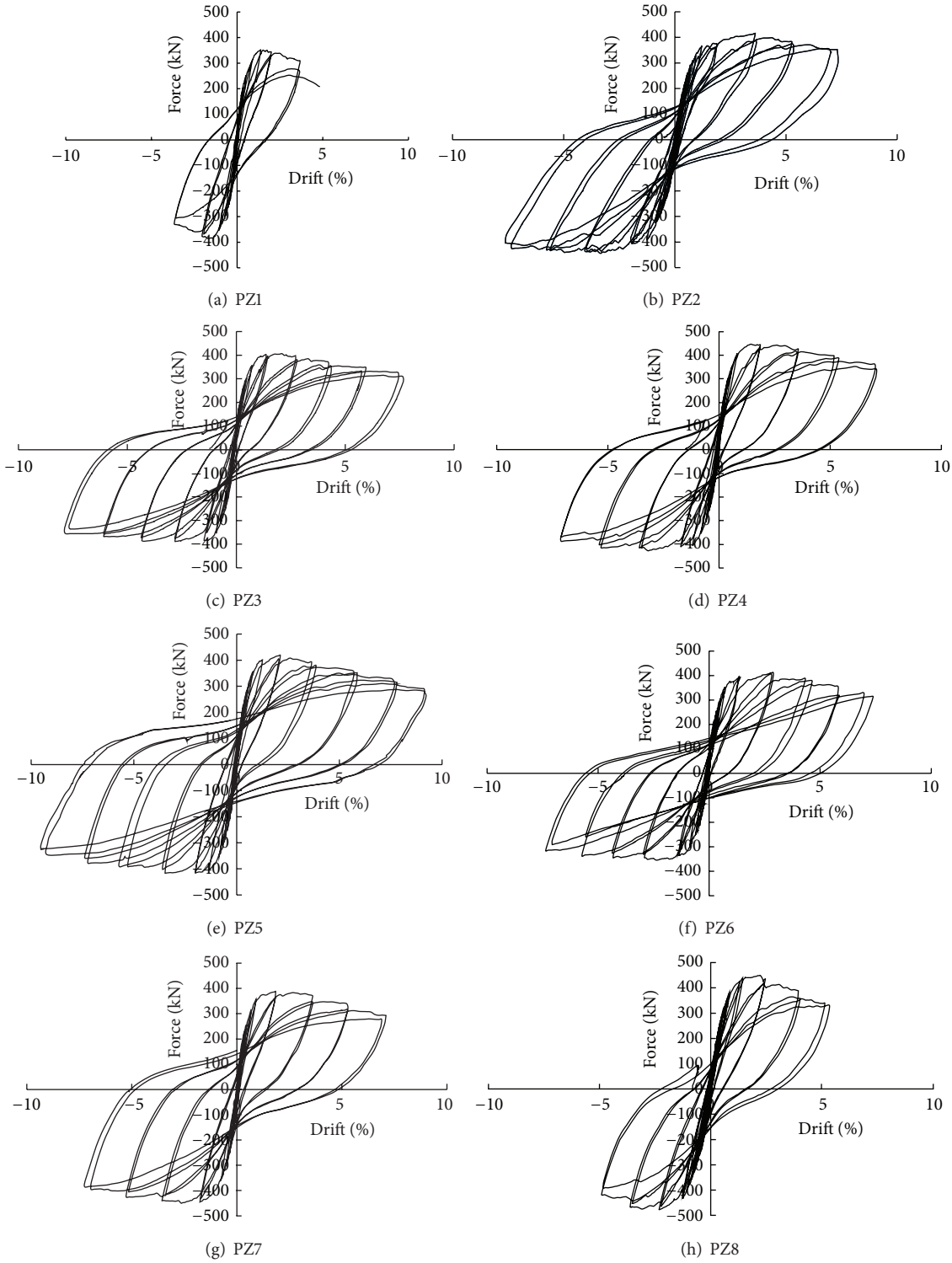

Figure 6: Typical force-drift hysteretic curves.

it is observed that seismic performance is more effectively improved for specimens with medium level prestressing.

3.5. Ductility Analysis. Ductility is an important parameter to determine the deformation capacity. In this paper ductility coefficient $\mu = \Delta_u/\Delta_y$ is used to measure the ductility of retrofitted columns. The ductility factor for each specimen is listed in Table 2.

From Table 2 it is observed that

(1) when the axial compression ratio and the strand configuration index are fixed, increasing the level

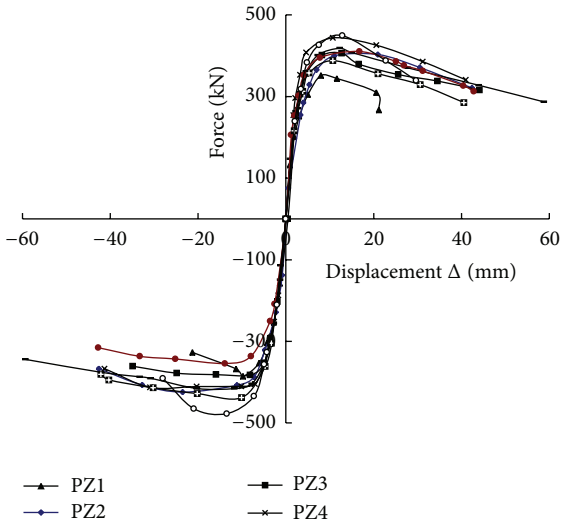

Figure 7: Skeleton curves of specimens.

of strand prestressing can improve the deformation capacity of the specimens. Compared with nonprestressed retrofitted specimen PZ2, the ductility coefficient of prestressed reinforced short columns PZ3 ($\alpha = 0.30$), PZ4 ($\alpha = 0.40$), and PZ5 ($\alpha = 0.50$) is increased by 18.9%, 26.8%, and 30.6%, respectively.

(2) Specimen PZ5 compared with PZ7, strand configuration index is doubled and ductility factor is increased by 27.3%. This is because other conditions are fixed, and confinement effect of core concrete increases with increase in steel strands configuration index.

(3) As axial compression ratio increases, the ultimate load increases, ultimate displacement decreases, the descending segment of the skeleton curve becomes steeper, bearing capacity of concrete members after ultimate load decreases rapidly, and deformation capacity reduces. Comparing PZ6 and PZ7; with equal strand configuration index and the prestressed level increased from $\alpha = 0.40$ to $\alpha = 0.50$, axial compression ratio increased from 0.60 to 0.81 and the displacement ductility index drops by 10.1%. Increasing axial compression ratio leads to increased height of compression zone, such that the cross section deformation capacity reduces. On the other hand, P-Δ effect increases due to high axial force. Deformation of the specimen after the maximum load is not stable and ductility worsens.

(4) Comparing the nonprestressed specimen PZ2 (with high strand configuration index, $\lambda_{sw} = 0.237$) with prestressed PZ7 (with low strand configuration index, $\lambda_{sw} = 0.119$), the displacement ductility index of PZ7 and PZ2 is 5.06 and 4.93, respectively.

(5) The strand configuration index of highly prestressed level specimen PZ8 is only 0.079. Compared with the control specimen, the ductility index of PZ8 is not significantly improved, indicating that in order to guarantee the retrofit effectiveness of high axial compression ratio, on the one hand strand configuration index should not be too small, and on the other hand strand prestressing level should be increased.

3.6. Stiffness Degradation. Secant stiffness $K_i = (|+P_i|+|-P_i|)/(|+\Delta_i| + |-\Delta_i|)$, which means the specimen ith secant stiffness is equal to the ratio of the sum of the ith load cycle's absolute maximum load values to sum of the corresponding absolute values of deformation. Divide the obtained values of each hystereses loop secant stiffness K_i by the yield stiffness K_y to get η_i, and the peak displacement Δ_i divided by the yield displacement Δ_y gives β_i. Relative stiffness degradation curves for each specimen are shown in Figure 8. We note the following.

(1) The relative stiffness degradation curves for all specimens generally have three stages: sharp decline of stiffness stage at initial loading, gradual stiffness degradation, and stiffness stabilizing stage.

(2) At initial loading ($\Delta < 3$ mm), prestressed, nonprestressed, and control specimens stiffness changes are basically the same: this is because, at initial loading deformation, internal cracks and cumulative damage are very small. At this stage stiffness of the short column depends on the cross-sectional area of the concrete column and strength of concrete.

(3) At descending stages, the stiffness degradation rate increases with increase in specimen axial compression ratio but decreases with increase in the strand configuration index and prestressing level, and when $\lambda_{sw} > 0.237$, the effect of α on stiffness degradation reduces.

4. Design for Column Retrofit

When the existing columns with insufficient shear resistance are subjected to seismic loading, the stirrups yield prematurely, causing the columns to undergo shear failure. Appearance of crossed cracks can be observed when the columns undergo stress reversals, and this will lead to damage of concrete. The external prestressed retrofitting by the strands plays the role of inhibiting the development of diagonal cracks, controlling of crack width, and also significantly increases the shear resistance, compression strength, and durability of the columns. It is therefore very clear that retrofitting by transverse prestressing strands significantly improves the bearing capacity of concrete columns and also promotes shear resistance.

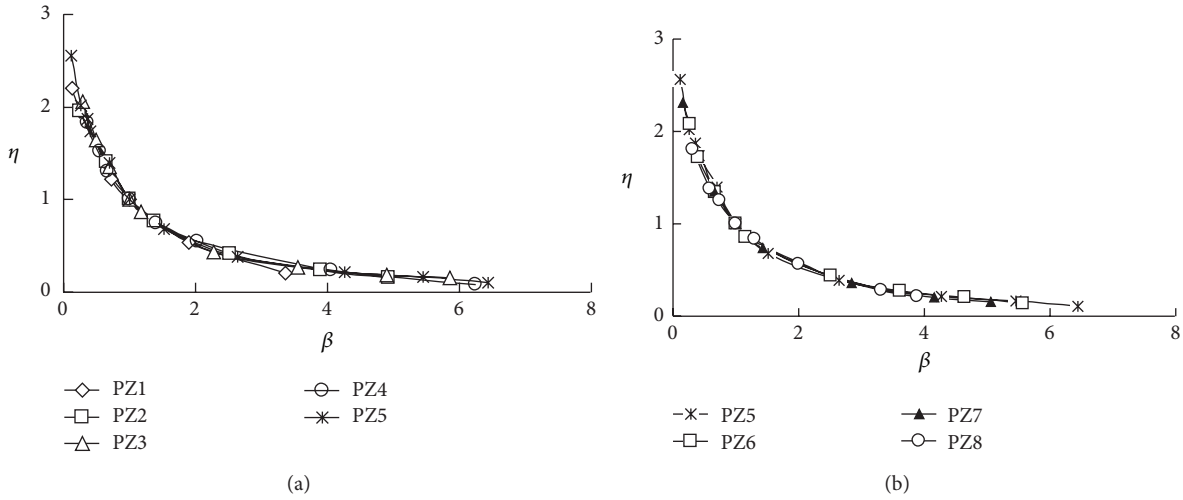

Figure 8: Relative stiffness degradation curves of specimens.

From the experiment results and analysis, a formula to calculate the shear capacity of prestressing strand retrofitted cylindrical concrete columns is proposed:

$$V_u = V_{cs} + V_{ps}, \tag{1}$$

$$V_{cs} = \frac{0.21}{\lambda} f_c D \overline{h}_0 + f_{yv} \frac{A_{sv}}{s} \overline{h}_0 + 0.07N, \tag{2}$$

$$V_{ps} = 2A_{ps} E_{ps} \left(\varepsilon_{pi} + \Delta\varepsilon_{pi}\right) \frac{D}{s_p}, \tag{3}$$

$$A_{ps} = \frac{\left(V - V_{cs}\right) s_P}{2E_{ps} D \left(\varepsilon_{pi} - \Delta\varepsilon_{pi}\right)}, \tag{4}$$

where V_{cs} is shear capacity of nonretrofitted columns (the shear capacity of concrete with stirrup reinforcement), which is calculated according to the proposed formula for circular cross section retrofitted concrete column, taking into account the current China design codes for concrete structures [12] and article [13], and considering the contribution of the axial force to the shear capacity value of $0.07N$, when $N > 0.8\pi f_c D^2/4$, take $N = 0.8\pi f_c D^2/4$, λ is the shear span ratio, f_{yv} is the design strength of the stirrups, f_c is the design axial compressive strength of concrete, and s is the spacing of the stirrups. V_{ps} is the shear capacity increment of retrofitted short concrete columns by prestressed steel strands. D is the column cross-sectional diameter and $\overline{h}_0$ is equivalent effective height h_0, that is, the distance from the center of gravity of all reinforcement bars to the edge of the compression zone in the other semicircle corresponding to the compression zone. $\overline{h}_0 = r + 2r_s/\pi$ (r is the radius of circular cross section, $r = D/2$; r_s is the radius of the circle in which the longitudinal reinforcement lies).

In formula (4), A_{ps} is the entire cross-sectional area of the strands in the same concrete cross section, E_{ps} is strand elastic modulus, ε_{pi} is strand initial pretensile strain, $\Delta\varepsilon_{pi}$ is strain increment of the strands at maximum horizontal bearing capacity relative to the initial strain, and s_p is strand spacing along the column height. When the prestressing strand spacing is too large, the confinement force applied to the concrete column is uneven and of smaller value, which causes early cracking of concrete, inhibiting the role of preventing concrete core cracks. Therefore $s_p \leq D/4$ is recommended.

Table 3: Comparison of calculation and test results.

Specimen number	V_{cs} (kN)	V_{ps} (kN)	V_u^t (kN)	V_u^c (kN)	V_u^t/V_u^c
PZ2	188.53	56.75	405.03	245.28	1.65
PZ3	188.53	192.95	419.30	381.48	1.10
PZ4	188.53	238.34	431.06	426.87	1.02
PZ5	188.53	218.35	419.80	406.88	1.03
PZ6	188.53	118.35	381.36	306.88	1.24
PZ7	188.53	141.73	408.94	330.26	1.24
PZ8	188.53	117.28	451.19	305.81	1.48

From the experiment it is found, when prestressed steel strand retrofitted specimen horizontal displacement is 20 mm (the ultimate displacement angle 1/29), specimen cracks are many and dense, wide through cracks are not formed, and the aggregates interlocking role is existent. When stirrups strain has reached yield value, the strand strain increment is greater than 2500 $\mu\varepsilon$. In this paper we recommend adopting the lower limit value of $\Delta\varepsilon_{pi}$ as 2500 $\mu\varepsilon$, which would be safety allowance left for the retrofitting designs.

In Table 3, V_{cs} is the shear capacity of concrete with stirrup reinforcement, the V_u^t and V_u^c are the experimental data and calculated results of total shear capacity, respectively. The average ratio between experimental and calculated value is 1.25, standard deviation 0.02. From Table 3 we see that, except for nonprestressed column PZ2, the predicted values are in good agreement with the experimental data for all prestressed columns.

5. Conclusion

(1) Prestressing strand retrofitting technology can significantly improve the seismic performance of short columns with large axial compression ratio and makes short columns failure pattern to change from shear failure to flexural-shear failure or flexural failure.

(2) Under high axial compression ratio from 0.60 to 0.90, the specimens still exhibit good ductility, indicating that the plastic deformation capacity of RC column is greatly improved by prestressed steel strands retrofitting.

(3) With the increase in horizontal displacement, the confinement function of stirrups and shear capacity is gradually shared by the steel strands. The higher the prestressed level and configuration index get, the earlier the steel strands get subjected to forces, and thus the greater the shear force is shared.

(4) The ductility of the specimen increases nonlinearly with increase in strand configuration index. When the strand configuration index increases to a certain value, there is slower increment of the ductility of the specimen with increase in configuration index; for RC column specimens with axial compression ratio greater than 0.80, a configuration index value not less than 0.237 is suggested.

(5) The retrofitted specimen magnitude of stiffness degradation increases with increase in axial compression ratio and decreases with increase in strand configuration index and prestressed level; when λ_{sw} is greater than a certain value, the effect of α on stiffness degradation reduces.

(6) A formula for shear capacity of prestressed steel strand retrofitted RC cylindrical columns is established, the calculated and experimental values agree well, and safety is guaranteed; it can be used for practical engineering designs.

Conflict of Interests

The authors declare that there is no conflict of interests regarding the publication of this paper.

References

[1] B. Andrawes, M. Shin, and N. Wierschem, "Active confinement of reinforced concrete bridge columns using shape memory alloys," *Journal of Bridge Engineering*, vol. 15, no. 1, pp. 81–89, 2010.

[2] M. A. Haroun and H. M. Elsanadedy, "Fiber-reinforced plastic jackets for ductility enhancement of reinforced concrete bridge columns with poor lap-splice detailing," *Journal of Bridge Engineering*, vol. 10, no. 6, pp. 749–757, 2005.

[3] A. Mirmiran and M. Shahawy, "Behavior of concrete columns confined by fiber composites," *Journal of Structural Engineering*, vol. 123, no. 5, pp. 583–590, 1997.

[4] M. T. Shahab and M. Hasan, "Experimental and analytical investigation of square RC columns retrofitted with Pre-stressed FRP strips," *University of Paris*, vol. 7, pp. 16–18, 2007.

[5] Z. H. Yan, C. P. Pantelides, and L. D. Reaveley, "Posttensioned FRP composite shells for concrete confinement," *Journal of Composites for Construction*, vol. 11, no. 1, pp. 81–90, 2007.

[6] H. Moghaddam, M. Samadi, K. Pilakoutas, and S. Mohebbi, "Axial compressive behavior of concrete actively confined by metal strips; part A: experimental study," *Materials and Structures*, vol. 43, no. 10, pp. 1369–1381, 2010.

[7] A. H. Munawarz and G. C. Robert, "Experimental study on the seismic performance of externally confined reinforced concrete columns," in *Proceedings of the 13th WCEE*, 2004.

[8] H. A. Moghaddam and M. Samadi, "Seismic Retrofit of large-scale reinforced concrete columns by prestressed high-strength metal strips," in *Proceedings of the Structures Congress (ASCE '09)*, pp. 2863–2872, May 2009.

[9] M. Saatcioglu and C. Yalcin, "External prestressing concrete columns for improved seismic shear resistance," *Journal of Structural Engineering*, vol. 129, no. 8, pp. 1057–1070, 2003.

[10] Z. C. Deng and J. P. Guo, "The new tensile and anchoring system for concrete column using external prestressing strands," Patent CN201010152467.X, 2010.

[11] J. Guo, Z. Deng, J. Lin, and H. Lu, "Experimental study of reinforced concrete slabs strengthened with prestressed high strength steel wire mesh," *China Civil Engineering Journal*, vol. 45, no. 5, pp. 84–92, 2012 (Chinese).

[12] GB50010-2010, *The Code for Design of Concrete Structures*, China Construction Industry Press, Beijing, China, 2010.

[13] X. Z. Zhou and W. S. Jiang, "Experimental study on the seismic behavior of short RC columns under high axial loading," *Xi'an University of Architecture and Technology*, vol. 6, pp. 103–106, 1985.